Biophysical Chemistry, 39 (1991) 69–78
Elsevier

BIOCHE 01526

Intensity and anisotropy decays of the tyrosine calmodulin proteolytic fragments, as studied by GHz frequency-domain fluorescence

I. Gryczynski [a], R.F. Steiner [b] and J.R. Lakowicz [a]

[a] *Department of Biological Chemistry, School of Medicine, University of Maryland (Baltimore), 660 W. Redwood Street, Baltimore, MD 21201 and* [b] *Department of Chemistry, University of Maryland (Baltimore County), 5401 Wilkens Avenue, Baltimore, MD 21228, U.S.A.*

Received 3 April 1990
Revised manuscript received 19 July 1990
Accepted 19 July 1990

Fluorescence; Anisotropy; Tyrosine; Calmodulin; Protein dynamics; Energy transfer; Ca^{2+}

Frequency-domain fluorescence measurements to 2 GHz were able to recover and account for essentially all of the intrinsic tyrosine anisotropy of calmodulin and its proteolytic fragments containing one or two tyrosine residues. Low-temperature measurements have detected a very rapid initial anisotropy decay in the 2-tyrosine species which may be attributed to radiationless energy transfer between the two tyrosines. The observed values of the rotational correlation times indicate that both tyrosines of calmodulin possess considerable mobility, which decreases in the presence of Ca^{2+} and at low temperatures.

1. Introduction

In an earlier publication, 200 MHz frequency-domain fluorescence data were presented for the tyrosine fluorescence of calmodulin and its proteolytic fragments [1]. Mammalian calmodulin contains two tyrosine residues at positions 99 and 138, and by cleavage at selective sites it is possible to obtain fragments which contain either one or both of these residues. The time dependence of the fluorescence intensities of calmodulin and the fragments was found to be multi-exponential and suggestive of a multiplicity of microenvironments sampled by the tyrosines, perhaps as a consequence of rotational mobility and/or hydrogen bonding. The time-dependent decay of anisotropy was also found to be multi-exponential and indicative of substantial tyrosine mobility. Both processes were, however, complicated by the presence of significant radiationless energy transfer between the two tyrosines, as reflected by a reduction of both the apparent limiting anisotropy at zero time and the static anisotropy measured at low temperatures.

Since the appearance of the above study, improvements in instrumentation have extended the range of accessible frequencies to 2 GHz [2]. This raises the possibility of monitoring processes too rapid to be detected with the earlier apparatus, including energy transfer. The present paper presents the findings obtained with the 2 GHz instrument. It has, in fact, proved possible to account for essentially all of the intrinsic anisotropy, including that component lost as a consequence of radiationless energy transfer between the tyrosines.

Correspondence address: J.R. Lakowicz, Dept of Biological Chemistry, School of Medicine, University of Maryland (Baltimore), 660 W. Redwood Street, Baltimore, MD 21201, U.S.A.

2. Experimental

2.1. Materials

Bovine calmodulin was isolated from frozen bull testes (Pel-Freez) by a method based on that

of Watterson et al. [3]. A further purification step was added using reverse-phase HPLC. The preparations used here were homogeneous by the criterion of acrylamide gel electrophoresis and had the expected amino acid compositions.

The proteolytic fragments TR1C (residues 1–77) and TR2C (residues 78–148 with two tyrosine residues) were isolated from a trypsin digest of bovine calmodulin in the presence of Ca^{2+} and purified according to published procedures [4–6]. The fragments TM1 (1–106) and TM2 (107–148) were isolated and purified from a thrombin digest of bovine calmodulin as described previously [5,6]. TM1 and TM2 each contain a single tyrosine residue.

The chemicals used were reagent grade, or better. The propylene glycol used was 'puriss' grade obtained from Fluka. Individual lots were inspected for background fluorescence, which was always less than 2% of sample fluorescence. All other solutions were made up using glass-redistilled water, and again the background did not exceed 2% under our experimental conditions. For static measurements, the background was subtracted. For dynamic measurements the background was ignored. The adequacy of the latter is indicated by the agreement between the limiting anisotropies of the single tyrosine molecules measured at $-60\,^{\circ}$C by static and dynamic methods.

2.2. Methods

The technique of frequency-domain fluorescence has been described in earlier publications [7–11]. Frequency-domain measurements were performed using the 2 GHz instrument which has been described elsewhere [2–11]. A train of 8-ps pulses from a cavity-dumped R6G dye laser, frequency doubled to 285 nm, provided the modulated excitation. The detector was a microchannel plate photomultiplier (Hamamatsu R1564 U). The emission was observed through a 305 nm interference filter.

The time decay of fluorescence intensity, $I(t)$, was fitted to the equation:

$$I(t) = \sum_i \alpha_i e^{-t/\tau_i} \tag{1}$$

where α_i and τ_i are the amplitude and decay time, respectively, of the i-th decay mode.

The time decay of fluorescence anisotropy, $A(t)$, was fitted to the equation

$$A(t) = \sum_i \beta_i e^{-t/\sigma_i} \tag{2}$$

where β_i and σ_i are the amplitude and correlation time, respectively, of the i-th decay mode. The amplitudes are related to the apparent limiting anisotropy at zero time, A_0, by

$$A_0 = \sum_i \beta_i \tag{3}$$

Depending upon the resolution of the instrument, the apparent value of $A_0 = \Sigma_i \beta_i$ may not be equal to the fundamental anisotropy observed at low temperature. In particular, poor resolution at short time coupled with an initial rapid decrease in the anisotropy can result in a lower apparent value for the anisotropy at $t = 0$. Energy transfer between adjacent fluorophores can result in a similar effect in the fundamental anisotropy observed at low temperature. In this case, the use of low temperature does not eliminate the origin of the decreased anisotropy, and one observes a decreased anisotropy due to depolarization during energy transfer.

3. Results

3.1. Fluorescence decay times

The fluorescence intensity decays were found to be multi-exponential at 5, 25 and 37°C for calmodulin and all of its tyrosine-containing fragments. In no case was it possible to obtain an acceptable fit in terms of a single component (table 1). This was the case for both the 1-tyrosine (TM1 and TM2) and the 2-tyrosine (TR2C)-containing fragments, indicating that the multiple decay modes do not arise solely from the different behavior of the two tyrosines, but must also reflect varying microenvironments sampled by the individual tyrosines as a consequence of their localized rotation, hydrogen bonding, energy transfer and/or different microenvironments. In most

cases, a significant improvement in χ_R^2 occurred upon increasing the number of assumed components from 2 to 3 (Table 1). While the recovered amplitudes and decay times adequately represent the data (fig. 1), this does not of course establish that only three discrete components are present. It is more likely that a distribution, perhaps multimodal, of decay times is present [12] and that the decay times cited in table 2 are actually poorly defined average quantities. While the values of the apparent decay times, as well as their overall averages, depend upon experimental conditions, the quantitative significance of the variation is uncertain, since they probably do not correspond to discrete decay components.

It is of interest that the multi-exponential character of the intensity decay persists at $-60\,^\circ$C in 70% propylene glycol (table 3) for both calmodulin and the single-tyrosine-containing fragments (TM1 and TM2). Thus, any immobilization of the tyrosine residues at low temperatures is not reflected by a return to exponential decay.

Table 1

Time decay of fluorescence intensity for calmodulin and TM1 [a]

Sample	Assumed no. of components	$\bar{\tau}$ (ns) [b]	τ_i (ns)	α_i	χ_R^2
Calmodulin	1		1.114	1	1565.1
	2		0.402	0.731	
			2.864	0.269	19.7
	3		0.352	0.674	
		2.657	2.087	0.299	
			7.179	0.0278	1.8
TM1	1		1.647	1	781.8
	2		0.274	0.544	
			2.397	0.456	7.3
	3		0.178	0.563	
		2.361	2.071	0.411	
			5.575	0.026	1.1

[a] The solvent was 0.05 M Mops, 5 mM EGTA (pH 6.5), 5 °C. The values of χ_R^2 were calculated using experimental uncertainties of 0.2° in phase and 0.005 in modulation.

[b] $\bar{\tau} = \Sigma\alpha_i\tau_i^2 = \Sigma f_i\tau_i$.

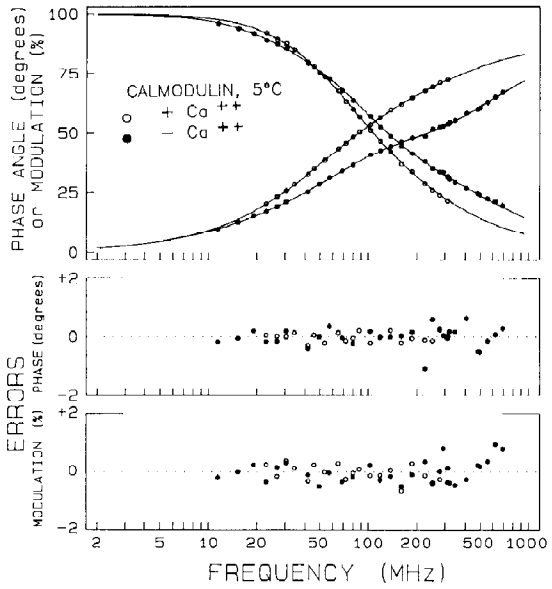

Fig. 1. (Upper) Frequency-domain data for the intensity decay of calmodulin at 5 °C in the absence (●) and presence (○) of Ca^{2+}. The buffer was 50 mM Mops (pH 6.5). Either 5 mM Ca^{2+} or 5 mM EGTA was present. The concentration of calmodulin was 6 μM. (Middle) Distribution of residuals for phase angle data. (Lower) Same, for modulation data.

3.2. Static anisotropies at $-60\,^\circ$C

Table 4 cites the static anisotropies, for excitation at 285 nm, of calmodulin and its fragments in 70% propylene glycol at $-60\,^\circ$C. The two thrombic fragments, TM1 and TM2, which each contain a single tyrosine, show anisotropies which are close to those found for *N*-acetyltyrosine amide and independent of Ca^{2+}. In contrast, calmodulin itself and its tryptic fragment TR2C, which contains both tyrosines, have static anisotropies which are substantially reduced over that of *N*-acetyltyrosine amide and which are, moreover, Ca^{2+}-dependent, the value of anisotropy decreasing significantly in the presence of Ca^{2+} (table 4).

Table 4 and fig. 2 also present comparative data on the anisotropies under these conditions of model compounds containing one and two tyrosines. The former include *N*-acetyltyrosine amide and Ala^5-dermorphin; the latter include Tyr-Tyr and dermorphin (fig. 2). In each case, the compound containing two tyrosines displays a static

Table 2

Decay times of fluorescence for calmodulin and its proteolytic fragments in aqueous solution [a]

Sample	Ca^{2+}	T (°C)	$\bar{\tau}$ (ns) [b]	α_1	τ_1	α_2	τ_2	α_3	τ_3	χ^2_R
Calmodulin	–	5	2.663	0.674	0.352	0.299	2.087	0.028	7.179	1.8
	–	25	2.358	0.673	0.295	0.296	1.791	0.021	7.111	1.0
	–	37	2.576	0.700	0.229	0.257	1.552	0.043	5.75	1.8
	+	5	2.701	0.318	0.716	0.628	2.579	0.054	5.075	0.5
	+	25	2.273	0.419	0.492	0.563	2.076	0.019	6.857	1.4
	+	37	2.118	0.548	0.453	0.371	2.311	0.08	3.105	1.0
TM1	–	5	2.361	0.563	0.178	0.411	2.071	0.026	5.575	1.1
	–	37	2.200	0.704	0.106	0.275	1.225	0.022	5.921	0.9
	+	5	3.811	0.486	0.269	0.397	2.582	0.123	6.105	1.2
	+	37	2.590	0.480	0.181	0.253	1.328	0.267	3.307	1.0
TM2	–	5	3.270	0.512	0.342	0.455	2.409	0.033	8.477	1.5
	–	37	2.138	0.635	0.205	0.347	1.616	0.018	6.672	1.0
	+	5	2.578	0.516	0.372	0.143	2.728	0.341	2.942	1.1
	+	37	2.386	0.572	0.164	0.343	1.836	0.085	4.011	1.2
TR2C	–	5	2.684	0.509	0.056	0.362	0.814	0.048	5.194	1.6
	–	37	2.476	0.799	0.115	0.177	1.097	0.024	5.900	1.2
	+	5	3.162	0.226	0.662	0.747	2.626	0.028	8.890	1.2
	+	37	2.465	0.593	0.384	0.384	2.108	0.023	7.121	1.5

[a] The solvent was 0.05 M Mops (pH 6.5). Either 5 mM Ca^{2+} (+) or 5 mM EGTA (−) was present. The concentrations were approx. 6 μM.

[b] $\bar{\tau} = \Sigma\alpha_i\tau_i^2 = \Sigma f_i\tau_i$.

anisotropy which is substantially reduced over the value for the corresponding single-tyrosine compound.

Both the 1- and 2-tyrosine compounds show a dependence of anisotropy upon wavelength (fig. 2). This is substantially more pronounced for the 2-tyrosine compounds. The wavelength dependence of the anisotropy for the single-tyrosine-containing species, including TM2, must arise from the presence of overlapping electronic transitions of tyrosine associated with different transition dipoles for absorption [13]. The most plausible explanation for the reduced anisotropies of the two tyrosine-containing molecules is in terms of radiationless energy transfer between the tyrosines. Edelhoch et al. [14] have demonstrated the occurrence of transfer in oligopeptides containing two tyrosines and shown that it results in a decrease in anisotropy. The enhanced wavelength dependence for the 2-tyrosine compounds may be attributed to the familiar 'red-edge' reduction in transfer efficiency with increasing wavelength which is characteristic of homologous donor-acceptor pairs. The failure of energy transfer upon red-edge excitation

Table 3

Decay times of fluorescence for calmodulin and model tyrosine-containing compounds at −60 °C [a]

Sample	α_1	τ_1 (ns)	α_2	τ_2 (ns)	α_3	τ_3 (ns)	χ^2_R
Calmodulin	0.764	0.910	0.112	4.38	0.124	15.14	1.7
NA-Tyr-A	0.264	0.80	0.736	4.45	–	–	1.5
Tyr-Tyr	0.185	0.51	0.815	4.16	–	–	1.3
TM2	0.636	0.43	0.260	2.60	0.104	15.47	1.2

[a] The solvent was 70% propylene glycol, 50 mM Mops (pH 6.5).

Table 4

Static anisotropies at −60 °C

Sample	Ca^{2+}	Anisotropy
Tyr-Tyr	−	0.186
Calmodulin	−	0.243
	+	0.211
TR2C	−	0.240
	+	0.216
N-Acetyltyrosine amide	−	0.315
TM1	−	0.289
	+	0.285
TM2	−	0.290
	+	0.286

[a] The solvent was 50 mM Mops (pH 6.5), 70% propylene glycol. Either 5 mM Ca^{2+} (+) or 5 mM EGTA (−) was present. The excitation wavelength was 285 nm; the emission wavelength was 305 nm.

occurs when the dipolar relaxation of the fluorophore environment is comparable to, or longer than the fluorescence lifetime. Under these conditions, those molecules are excited which have a minimal energy separation between ground and excited state. Since there is no additional dipolar relaxation on a time scale comparable to the fluorescence decay time, the minimal energy separation between excited and ground-state molecules persists during the excited state, with a resultant reduction in effective overlap integral and transfer efficiency [15].

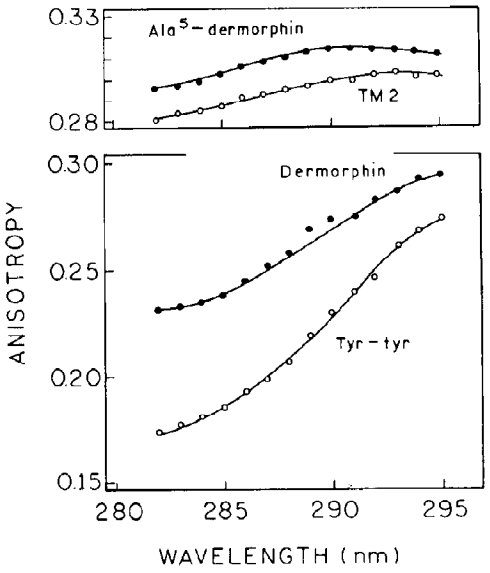

Fig. 2. (Upper) Static anisotropies at −60 °C as a function of wavelength for a series of 1-tyrosine molecules. The solvent was 50 mM Mops (pH 6.5), 70% propylene glycol. The wavelength of emission was 305 nm. (Lower) Same, for 2-tyrosine species.

3.3. Dynamic anisotropies at −60 °C

At −60 °C in 70% propylene glycol, the anisotropy decay of the single-tyrosine model compounds and the single-tyrosine fragment TM2 could be adequately described in terms of a single rotational mode corresponding to an elevated correlation time (table 5). The apparent zero time values of anisotropy were, as expected, close to the static anisotropy values. Apparently, a very slow molecular rotation persists in this highly viscous medium. However, it should be noted that the short decay time of tyrosine precludes an accurate measurement of long correlation times, so that the values in table 5 should be regarded as lower limits to the actual correlation times. There is, however, no indication of a rapid decay mode for the anisotropy.

The behavior is different for calmodulin and the model compound Tyr-Tyr. In neither case could the anisotropy decay be described adequately in terms of a single decay mode. In both

Table 5

Dynamic anisotropies at −60 °C [a]

Sample	β_i [b]	σ_i [b] (ns)	A_0 [c]	χ_R^2
Acetyltyrosine amide	0.304	157.9	0.304	1.2
Tyr-Tyr	0.242	40.1	0.242	19.5
	0.048	0.3		
	0.232	75.2	0.280	1.2
TM2	0.286	259.4	0.286	0.7
Calmodulin	0.267	61.5	0.267	56.4
	0.049	1.0		
	0.239	1145.3	0.288	1.8

[a] The solvent was 0.05 M Mops (pH 6.5), 70% propylene glycol. In the cases of calmodulin and TM2, 5 mM EGTA was present.

[b] Amplitudes, β_i, and rotational correlation times, σ_i, which provide an optimal fit to the time decay of anisotropy assuming one or two components.

[c] Computed limiting anisotropies; $A_0 = \sum_i \beta_i$.

cases, a very rapid initial decline of anisotropy was superimposed upon a very slow subsequent decay, presumably corresponding to global rotation of the molecule or limited resolution of our data for the longer correlation time. The summed amplitudes of the two rotational modes are similar in magnitude to the apparent zero time anisotropies of the single tyrosine compounds and to the corresponding static anisotropies of these same compounds (0.29 ± 0.01). Thus, essentially all the limiting anisotropy can be recovered by measurements extending to 2 GHz.

The initial decay of anisotropy for the 2-tyrosine compounds is too rapid (0.3–1 ns) for any plausible rotation under these conditions. The most probable explanation is that it reflects radia-

Table 6

Dynamic anisotropies at ordinary temperatures, analyzed with floating values of A_o [a]

Sample	Ca^{2+}	T (°C)	β_1	σ_1 (ns)	σ_1^{25} (ns) [b]	β_2	σ_2 (ns)	σ_d^{25} (ns) [b]	χ_R^2
Calmodulin	–	5	–	–	–	0.251	2.52	1.38	11.4
			0.047	0.09	0.05	0.238	2.88	1.57	0.8
		25	–	–	–	0.234	1.69	1.69	11.6
			0.084	0.08	0.08	0.212	2.03	2.03	0.6
		37	–	–	–	0.215	0.97	1.31	24.1
			0.115	0.07	0.09	0.179	1.35	1.81	0.7
	+	5	–	–	–	0.232	4.47	2.44	17.5
			0.071	0.95	0.52	0.175	8.41	4.60	1.0
		25	–	–	–	0.242	3.28	3.28	22.8
			0.074	0.47	0.47	0.194	5.43	5.43	1.7
		37	–	–	–	0.242	2.38	3.18	39.0
			0.077	0.25	0.33	0.201	3.61	4.83	1.5
TM1	–	5	–	–	–	0.176	1.34	0.73	41.9
			0.215	0.08	0.04	0.123	2.47	1.35	0.8
		37	–	–	–	0.235	0.28	0.37	10.0
			0.253	0.06	0.08	0.111	0.55	0.74	0.6
	+	5	–	–	–	0.201	4.29	2.35	47.9
			0.100	0.17	0.09	0.175	6.52	3.57	1.2
		37	–	–	–	0.248	2.16	2.90	37.6
			0.074	0.17	0.22	0.217	2.88	3.85	1.2
TM2	–	5	–	–	–	0.195	0.86	0.47	30.0
			0.197	0.22	0.12	0.086	2.42	1.32	0.6
		37	–	–	–	0.343	0.19	0.25	1.4
			0.157	0.15	0.20	0.192	0.22	0.29	1.4
	+	5	–	–	–	0.241	4.90	2.68	22.8
			0.067	0.19	0.10	0.220	6.27	3.43	0.9
		37	–	–	–	0.233	1.18	1.58	63.8
			0.17	0.20	0.27	0.144	2.47	3.31	1.5
TR2C	–	5	–	–	–	0.272	1.57	0.86	29.5
			0.099	0.09	0.05	0.238	2.07	1.13	1.2
		37	–	–	–	0.272	0.84	1.12	13.9
			0.112	0.07	0.10	0.227	1.08	1.44	1.5
	+	5	–	–	–	0.246	4.09	2.24	12.5
			0.049	0.35	0.19	0.225	5.04	2.76	1.4
		37	–	–	–	0.259	1.77	2.38	4.9
			0.053	0.25	0.33	0.231	2.05	2.74	0.7

[a] The solvent was 50 mM Mops (pH 6.5), plus either 5 mM EGTA or 5 mM Ca^{2+}. The wavelengths of excitation and emission were 285 and 305 nm, respectively.

[b] This quantity is the measured correlation time (ϕ^T) corrected to the standard conditions of H_2O, 25 °C by the equation $\phi^{25°C} = \phi^T(T/\eta)_T/(T/\eta)_{25°C}$, where T is the absolute temperature and η the viscosity.

tionless energy transfer between the two tyrosines. The apparent limiting anisotropies corresponding to the slower rotational modes are comparable in magnitude to the static anisotropies (tables 4 and 5).

3.4. Dynamic anisotropies at higher temperatures

At pH 6.5 the anisotropy is multi-exponential for calmodulin and all of its proteolytic fragments (tables 6 and 7; fig. 3). In no case was it possible to obtain an acceptable fit in terms of a single rotational mode. The decay was multi-exponential at 5, 25 and 37 °C in both the absence and presence of Ca^{2+}. In each case the anisotropy could be adequately described in terms of two rotational modes, the more rapid of which corresponds to a subnanosecond correlation time and presumably arises from some form of internal rotation upon which the effects of energy transfer are superimposed for the 2-tyrosine molecules. The slower rotational mode has a correlation time of several nanoseconds and reflects a more global motion of the molecules.

Dynamic anisotropies were determined from the frequency-domain data. Data for calmodulin in the absence and presence of Ca^{2+} are shown in figs 3 and 4, respectively. The data typically dis-

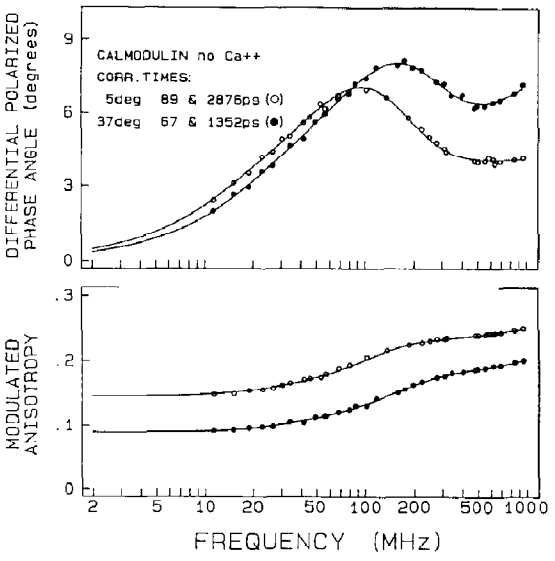

Fig. 3. Frequency-domain anisotropy data for calmodulin at 5 °C (○) and 37 °C (●), in the absence of Ca^{2+}. The solid lines show the best two-correlation-time fits (table 6).

Table 7

Dynamic anisotropies at ordinary temperatures, analyzed with a fixed value of A_0 [a]

Sample	Ca^{2+}	T (°C)	g_1	σ_1 (ns)	σ_1^{25} (ns)	g_2	σ_2 (ns)	σ_2^{25} (ns) [b]	χ_R^2
Calmodulin	−	5	0.176	0.08	0.04	0.824	2.86	1.56	0.8
	−	25	0.271	0.09	0.09	0.729	2.04	2.04	0.6
	−	37	0.386	0.07	0.09	0.614	1.36	1.82	0.7
	+	5	0.238	0.16	0.09	0.762	5.46	2.98	7.1
	+	25	0.268	0.26	0.26	0.732	4.73	4.73	1.7
	+	37	0.281	0.21	0.28	0.719	3.50	4.69	1.7
TM1	−	5	0.588	0.11	0.06	0.412	2.57	1.41	0.9
	−	37	0.345	0.12	0.16	0.655	0.70	0.94	1.0
	+	5	0.384	0.15	0.08	0.616	6.44	3.52	1.2
	+	37	0.245	0.20	0.26	0.755	2.92	3.91	1.3
TM2	−	5	0.695	0.20	0.11	0.305	2.36	1.29	0.6
	−	37	0.568	0.24	0.32	0.432	0.24	0.32	8.6
	+	5	0.230	0.20	0.11	0.770	6.29	3.44	0.9
	+	37	0.545	0.29	0.38	0.455	2.78	3.73	2.3
TR2C	−	37	0.325	0.25	0.33	0.675	1.21	1.62	3.4
	+	5	0.198	0.24	0.13	0.802	4.90	2.68	1.5
	+	37	0.187	0.24	0.32	0.813	2.04	2.73	0.7

[a] Conditions were the same as for table 6. Values of A_0 were fixed at 0.29 for all species in the absence of Ca^{2+}; at 0.285 for calmodulin, TM1 and TR2C in the presence of Ca^{2+}; and at 0.286 for TM2 in the presence of Ca^{2+}.

[b] See footnote [b] of table 6.

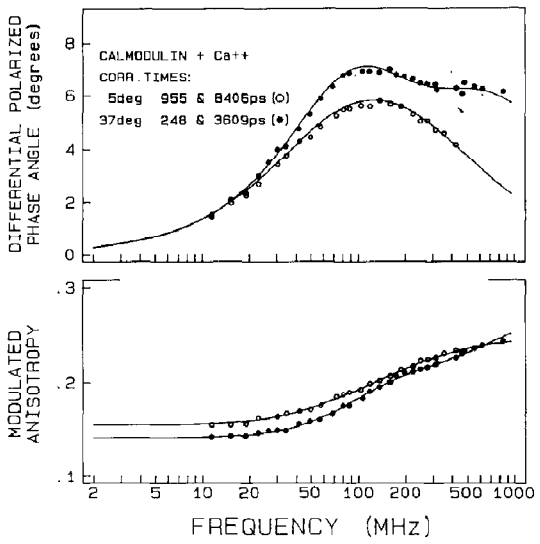

Fig. 4. Frequency-domain anisotropy data for calmodulin at 5°C (○) and 37°C (●), in the presence of Ca^{2+}. The solid lines show the best two-correlation-time fit (table 6).

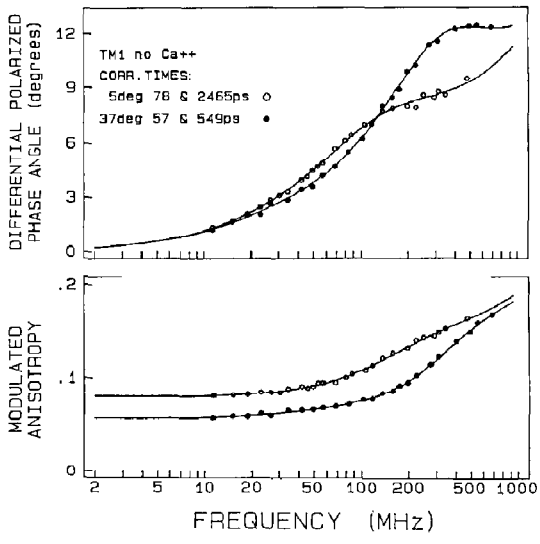

Fig. 5. Frequency-domain anisotropy data for calmodulin fragment TM1 at 5°C (○) and 37°C (●), in the absence of Ca^{2+}.

play a maximum in the differential phase angles near 100 MHz, which is due dominantly to global protein rotation. Additionally, the phase angles increase at higher frequencies, which is due to the subnanosecond components in the anisotropy decay. It is interesting to note that these high-frequency components appear to increase in amplitude at higher temperatures, which reflects an increased amplitude for the rapid portion of these anisotropy decays. Additionally, the amplitudes of the short components appear to be decreased by the presence of Ca^{2+}. The anisotropy decays of TR2C were found to be similar to those of calmodulin (tables 6 and 7).

The frequency-domain anisotropy data for the fragments (figs 5 and 6) are visually distinct from those observed for intact calmodulin. The differential phase data for the fragments show considerably less amplitude near 100 MHz, and increased amplitude at higher frequencies. These data reflect a substantially greater amplitude of the rapid portion of the anisotropy decay for these single-tyrosine fragments.

The anisotropy decay data were analyzed in two ways. In the first of these, the amplitudes were allowed to float freely, without restriction upon either their individual values or their sum (table 6). In the second, the sum of the amplitudes, which was equal to A_0, was fixed at a value close to that expected for an immobilized single-

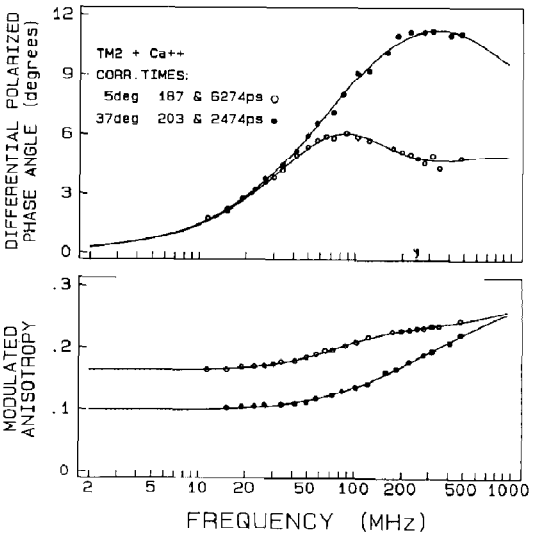

Fig. 6. Frequency-domain anisotropy data for calmodulin fragment TM2 at 5°C (○) and 37°C (●), in the presence of Ca^{2+}.

tyrosine-containing molecule (table 7). In this case the equivalent of eq. 2 is

$$A(t) = A_0 \sum_i g_i e^{-t/\sigma_i} \quad (4)$$

where g_i is the relative amplitude and $\Sigma_i g_i = 1$.

The values of the rotational correlation times recovered by the two approaches are essentially equivalent, as are the values of χ^2_R, with one exception (tables 6 and 7). The high quality of the fits with the fixed values of A_0 suggests that essentially all of the anisotropy is being recovered by measurements with the 2 GHz instrument, including that portion which decays rapidly because of energy transfer (fig. 3). In contrast, the earlier measurements with the 200 MHz instrument yielded apparent values of A_0 which were reduced for the 2-tyrosine species and close to their static values [1].

When the values of A_0 were allowed to float, there was somewhat more scatter in the apparent values obtained (table 6). However, the apparent values were scattered about that expected in the absence of transfer and there was no systematic difference between the 1- and 2-tyrosine molecules. It is probable that the rotational mode corresponding to the shorter correlation time arises in part from inter-tyrosine energy transfer in the case of the 2-tyrosine species. However, this is unlikely to be the sole origin, since the 1-tyrosine fragments also show a subnanosecond correlation time. It is noteworthy that there is no major systematic difference in the magnitude of the shorter correlation time between the 1- and 2-tyrosine molecules, although the latter presumably correspond to averages of times arising from transfer and rotation. This is in contrast to the behavior at $-60\,^\circ$C, where a short correlation time is observed only for the 2-tyrosine molecules (table 5). It is probable that, at the higher temperatures, the distinction is blurred between anisotropy decay due to transfer and to rotation by other factors, including differences in mobility between Tyr-99 and Tyr-139, effects of fragmentation upon mobility, as well as experimental scatter.

The magnitude and relative amplitude of the longer correlation time are sensitive to conditions, as is also the average correlation time. The average correlation time generally increases in the presence of Ca^{2+} and at low temperatures, as does the relative amplitude of the slower rotational mode, in conformity with the results obtained at 200 MHz [1]. In the case of TM2 at 37 °C in the absence of Ca^{2+}, the slower decay mode appears to be lost (table 6); there is no improvement in fit upon assuming two rather than one component. The implication is that organized structure is largely lost for the TM2 fragment under these conditions.

4. Discussion

These results indicate that it is possible with the 2 GHz variable-frequency phase fluorometer to account for essentially all of the fluorescence anisotropy decay of the two tyrosines of calmodulin and that this anisotropy decay contains a significant component arising from radiationless energy transfer between the tyrosines. If the mutual orientation of the two is random, the sensitized tyrosine emission will be depolarized, resulting in a shorter correlation time for this component in the emission. For both native calmodulin and the 2-tyrosine fragment TR2C, the effect appears to be more important for the Ca^{2+}-ligated species, suggesting that the separation of the two tyrosines is smaller than for the apo-protein.

The existence of significant transfer is consistent with the positions of the tyrosines in the crystallographic structure [16]. These residues (Tyr-99 and Tyr-138) appear to be approx. 15 Å apart, which is comparable to the Förster distance for phenol-to-phenol energy transfers of 16 Å [17].

A substantial localized mobility of both Tyr-99 and Tyr-138 is shown by the two thrombic fragments, TM1 and TM2, which contain only Tyr-99 and Tyr-138, respectively. Moreover, the mobility of both tyrosines decreases sharply in the presence of Ca^{2+}, indicating that Ca^{2+} ligation confers increased structural rigidity on either half of the C-terminal lobe, even though only a single binding site is present. An increase in temperature from 5 to 37 °C appears to increase the tyrosine mobility for both thrombic fragments, whether or not Ca^{2+} is present. At 37 °C in the absence of Ca^{2+}, the

magnitudes of both correlation times for both TM1 and TM2 are so small as to suggest that few structural restraints persist for the rotation of the tyrosine. In contrast, for native calmodulin under the same conditions, the rotation of the tyrosines appears to be substantially hindered, as indicated by the magnitude of the correlation time.

Qualitatively, the effects of temperature and Ca^{2+} ligation are similar for native calmodulin and the fragments. While interpretation of the short correlation time is complicated by the presence of transfer, the magnitude of the longer correlation time clearly increases in the presence of Ca^{2+}. However, even in the presence of Ca^{2+}, the magnitude of the longer correlation time is too short to be compatible with the global rotation of a rigid molecule with the crystallographic structure.

Small and Anderson [18], using a calmodulin derivative in which Tyr-99 and Tyr-138 were covalently linked, found correlation times corresponding to global rotation of 6.5 and 9.9 ns in the absence and presence of Ca^{2+}, respectively. In the absence of Ca^{2+}, a second, more rapid rotational mode was also present. While these results are qualitatively consistent with the findings reported here, the magnitudes of the longer correlation times are much higher and the amplitudes of the more rapid rotational mode much smaller than for native calmodulin. This may logically be attributed to the effects of cross-linking Tyr-99 and Tyr-138, which would tend to block localized rotation and cause the tyrosines to rotate as a unit. Since the two tyrosines are now effectively a single fluorophore, energy transfer is not a factor.

Kilhoffer et al. [19], using the mutant calmodulin VU-9, in which a tryptophan group replaces Tyr-99, found from static polarization measurements values of 3.0 and 4.7 ns for the long correlation time in the absence and presence of Ca^{2+}, respectively. These values are comparable to those reported here for the tyrosine fluorescence of calmodulin.

Acknowledgements

Supported by grants GM-35154 (J.R.L.) from the National Institutes of Health and DMB-8502835 and DMB-8511065 (J.R.L.) from the National Science Foundation. This work was performed using the facilities at the Center for Fluorescence Spectroscopy (NSF DIR-8710401). J.R.L. acknowledges the support of the Medical Biotechnology Center, University of Maryland.

References

1 I. Gryczynski, J.R. Lakowicz and R.F. Steiner, Biophys. Chem. 30 (1988) 49.
2 J.R. Lakowicz, G. Laczko, I. Gryczynski, H. Cherek and W. Wiczk, SPIE Proc. 909 (1988) 15.
3 D.M. Watterson, F. Sharief and T.C. Vanaman, J. Biol. Chem., 255 (1980) 962.
4 H. Brzeska, J. Szynkiewicz and W. Drabikowski, Biochem. Biophys. Res. Commun. 115 (1983) 87.
5 D. Guerini, J. Krebs and E. Carafoli, J. Biol. Chem. 259 (1984) 15172.
6 D.L. Newton, M.D. Oldewurtel, M.H. Krinks, J. Shiloach and C.B. Klee, J. Biol. Chem. 259 (1984) 4419.
7 J.R. Lakowicz and B.P. Maliwal, Biophys. Chem. 21 (1985) 61.
8 J.R. Lakowicz, H. Cherek, B.P. Maliwal and E. Gratton, Biochemistry 24 (1985) 376.
9 J.R. Lakowicz, G. Laczko, H. Cherek, E. Gratton and M. Limkeman, Biophys. J. 46 (1984) 463.
10 E. Gratton, M. Limkemann, J.R. Lakowicz, B.P. Maliwal, H. Cherek and G. Laczko, Biophys. J. 46 (1984) 479.
11 J.R. Lakowicz, G. Laczko and I. Gryczynski, Rev. Sci. Instrum., 57 (1986) 2499.
12 B.D. Wagner, D.R. James and W.R. Ware, Chem. Phys. Lett. 138 (1987) 181.
13 G. Weber, Biochem. J. 75 (1960) 335.
14 H. Edelhoch, R.L. Perlman and M. Wilchek, Biochemistry 7 (1968) 3893.
15 A.P. Demchenko, Ultraviolet spectroscopy of proteins (Springer, Berlin, 1986) p. 183.
16 Y.S. Babu, J.S. Sack, T.G. Greenbough, C.E. Bugg, A.R. Means and W.J. Cook, Nature 315 (1985) 37.
17 G. Weber, in: Fluorescence and phosphorescence analysis, ed. D.M. Hercules (Wiley, New York, 1965) Ch. 8, p. 217.
18 E.W. Small and S.R. Anderson, Biochemistry 27 (1988) 419.
19 M.C. Kilhoffer, D.M. Roberts, A. Adibi, D.M. Watterson and J. Haiech, Biochemistry 28 (1989) 6086.